BUTTERWORTH HEINEMANN

Polymer Vol. 36 No. 10, pp. 1957–1968, 1995

0032-3861/95/$10.00 + 0.00

Sheet formation in immiscible polymer blends: model experiments on initial blend morphology

Uttandaraman Sundararaj*, Yoav Dori and Christopher W. Macosko
Department of Chemical Engineering and Materials Science, University of Minnesota, Twin Cities, Minneapolis, MN 55455, USA
(Received 15 July 1994; revised 28 September 1994)

Model experiments were performed to determine the controlling parameters in the evolution of the phase morphology of immiscible polymer blends from pellets to micrometre-sized particles. It has been established that during melting in both twin-screw extruders and batch mixers, the dispersed phase is stretched into sheets. These sheets develop into cylinders and the cylinders ultimately break into spherical droplets via Rayleigh-type instabilities. Here, we show that micrometre thick sheets can be created from millimetre-sized pellets by shearing in the parallel discs geometry. Extensional flow is not required to generate the sheets. Pellets are seen to break up in three ways: (1) by stretching into cylinders with drops streaming off the end; (2) by extending sheets that form fingers at the edges; and (3) by stretching into thin sheets that break up by forming holes. A map of the different regions of breakup is given using the Deborah number and the ratio of the first normal stress difference of the matrix to the restoring stress of the pellet (drop). The drop-restoring stress is the sum of the surface stress resulting from interfacial tension and the first normal stress difference of the drop. The masterplot explains why sheets can be easily formed from large drops and gives a window where the sheets are stable and do not form holes.

(Keywords: polymer blends; mixing; breakup mechanisms)

INTRODUCTION

Blends are prepared in several ways but the most common method is to combine pellets of two (or more) components in an intensive mixer, typically a twin-screw extruder. Since the final morphology affects the properties of the blend, the morphology of the material exiting the mixer has been studied[1–16]. However, it is important to uncover the mechanisms of drop breakup during the important initial softening/mixing step to gain a fundamental understanding of the process. The major morphological changes during polymer blending occur during the initial softening stage[1–10] when pellets are stretched into sheets[7–10]. This paper shows how morphology develops in polymer/polymer melt blends. In this work, factors which influence sheet formation (matrix and dispersed phase material properties, flow field, interfacial properties) are investigated and the transitions between different types of breakup are found. Guidelines are established to predict when sheets will be stable against breakup. These rules are important, for example, when it is desirable to have one component dispersed as sheets inside another component. This can result in a blend with improved barrier properties[17–19] since the component dispersed as sheets can decrease the permeability considerably.

*To whom correspondence should be addressed at present address: Department of Chemical Engineering, University of Alberta, 536 Chemical-Mineral Engineering Building, Edmonton, Alberta, Canada

Work on morphology development during the mixing process has been performed in detail only over the past four years[2–8,10], and many issues still remain unresolved. Researchers have used batch mixers and varied the mixing time[2,3,7,8] or have used extruders and varied the mixing length[5,6,8]. Plochocki *et al.*[3] postulated that an 'abrasion' mechanism was responsible for the quick morphology development in the initial melting or softening stage. They speculated that there was abrasion (similar to rubber abrasion) between the two types of pellets and between the pellets and the wall. However, our group has shown that sheets are formed in blends during the initial melting stage[7,8].

Previous work and motivation

In our previous work[8], we showed the morphology development in industrial twin-screw mixers. Blend systems were chosen so that the dispersed phase was resistant to a solvent which would dissolve the matrix phase. The most significant morphology development in a corotating twin-screw extruder occurred in the first two kneaders in the first kneading section, and that in the batch mixer occurred within 1.0 min. The sheet structures isolated by extracting the matrix phase are shown in *Figure 1*. After the initial breakup, the particle size is not reduced significantly.

To show that the sheet structure was not due to the solvent extraction procedure, we pre-melted and then blended a single PP3050 pellet inside a PS666D matrix

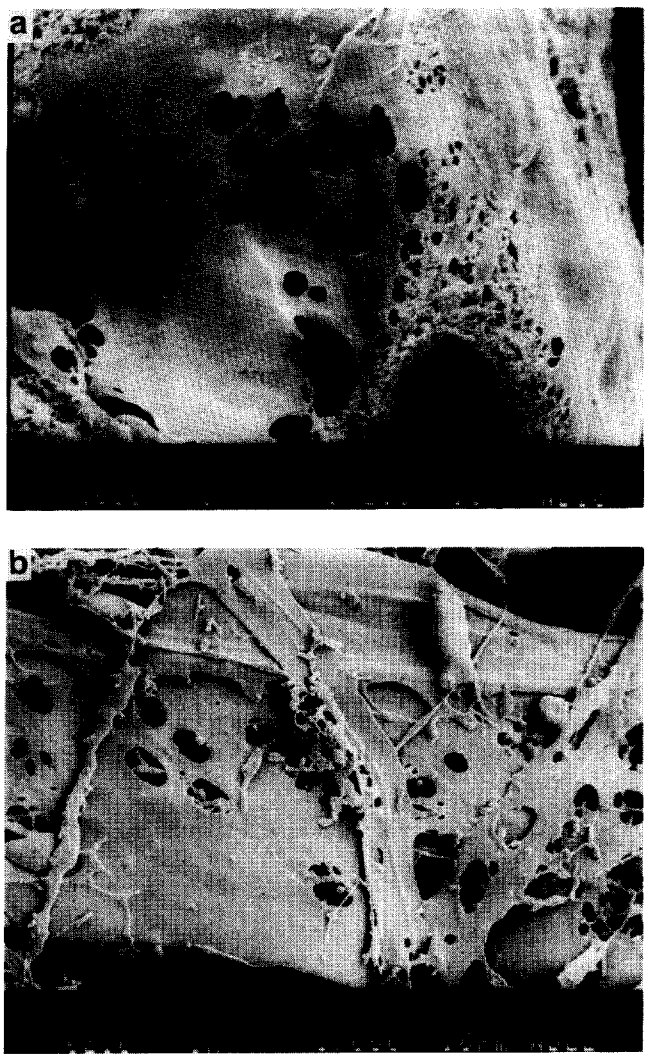

Figure 1 Scanning electron microscopy (SEM) micrographs of the initial morphology in polymer blends. In both micrographs, the polystyrene matrix phase has been extracted with methylene chloride. (a) The PS666D/PP3050 system in a twin-screw extruder. A sheet of PP with holes is seen at the first point of melting in the extruder. (b) The PS666D/PA330 system in a batch mixer at 1.0 min of mixing. Sheets of PA330 are seen. Both runs were performed at a mixer temperature of 200°C, a maximum mixer shear rate of 65 s^{-1} and with a matrix to dispersed phase concentration ratio of 80/20

in the batch mixer (see *Table 1* for polymer properties). The single PP pellet and 52.5 g of PS pellets were placed in the mixer and heated to 200°C. The mixture was held at 200°C without shearing for 3 min. The molten mass was sheared for 2 s after which the mixer was opened and the blend was quenched in liquid nitrogen. The quenching time was less than 30 s. The blend sample was viewed via optical microscopy without using solvent. The lacey sheets of PP seen through the transparent PS matrix are shown in *Figure 2*. We can see how the coalescence of the holes in the sheet can produce drop micrometres in size. The holes form at the front edge of the sheet as it is being pulled. The sheet is thinner at the front edge.

Cylinders are formed when the holes in the sheet coalesce[8] or when the edges of ribbons are pulled together by interfacial tension. The cylinders break up owing to Rayleigh-type wave instabilities resulting in spherical drops. Interfacial tension is relatively low in polymer systems (~ 5 mN m^{-1}), and therefore it is anticipated that the low interfacial tension will not have a large effect on drop breakup until the matrix stresses are about equal to the interfacial stresses. Using shear stresses found in industrial mixers ($\sim 10^4$ Pa)[20], this is predicted to occur for polymer blends when the drop size is about 1 μm.

Here we perform model experiments using the rotating parallel discs flow geometry to investigate the breakup of a single polymer pellet dispersed inside a matrix of another polymer. We construct a map showing the different regions of breakup. The effect of reaction on sheet formation and breakup is investigated. It was of interest to see if the 'sheeting' mechanism seen in batch mixers and twin-screw extruders would also be present in the simple shear flow between parallel discs.

BACKGROUND

Liquid sheet breakup

Most of the work performed on disintegration of flowing liquid sheets revolves around sheets of Newtonian liquids formed from nozzles. These sheets break up via wave instabilities due to air friction. Liquid sheets have also been seen to break up through hole formation. Dombrowski and Fraser[21] photographed the disintegration of sheets of several liquids. They saw breakup caused by waves produced by air friction but also saw perforations in the sheet for several liquid systems. Holes have been seen in other studies but have been overlooked[22,23]. When Dombrowski and Fraser used particles in liquids, they saw that wettable particles had no effect on the breakup mechanism, but unwettable particles caused perforations in the sheet. The perforations occurred at some distance from the nozzle as the sheet thinned when it moved further away from the nozzle. When larger unwettable particles were used, holes occurred in the sheet closer to the nozzle. For holes to form, the two surfaces of the sheet must touch. It was inferred that the particle bridged the gap between the two surfaces of the sheet[24] and created a hole that enlarged owing to the surface tension effects[25]. Holes were also observed in a

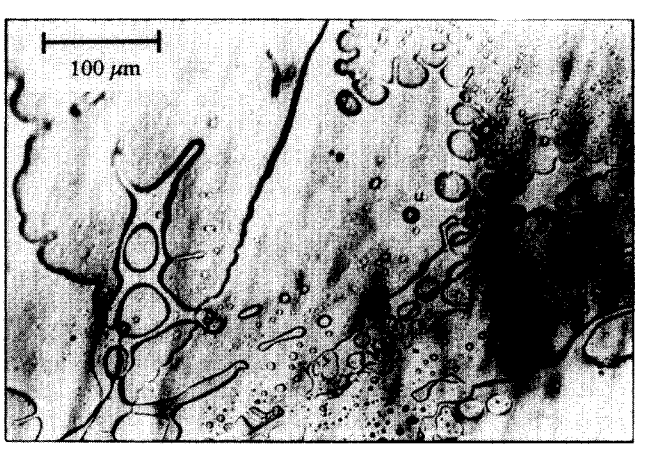

Figure 2 Optical micrograph showing a single PP3050 pellet in a PS666D matrix. The pellet has broken into sheets and drops within 2 s of blending in the batch mixer. The PP sheets are seen through the PS matrix without the need for dissolution of the matrix. The edges of the sheets, which should be thinner, have many holes which have coalesced to give a lacey structure. Micrometre-sized droplets are present after only 2 s of blending. This is the same system that is shown in *Figure 1a*. Side lighting was used to get better contrast between the phases

Table 1 Flow properties of polymers at 200°C

Polymer (abbreviation)	Molecular weight (M_w) (supplier)	Zero shear viscosity (kPa s)	G' at 2 s^{-1} (kPa)	Characteristic relaxation time λ (s)
Polystyrene-1 (PS666D)	200000 (Dow)	9.5	5.4	0.64
Polystyrene-2 (PS615)	175000 (Dow)	3.7	1.8	0.31
Poly(methyl methacrylate) (PMMA)	110000 (Rohm and Haas)	60	35	1.25
Polypropylene-1 (PP3050)	60000 (Elf Atochem)	6	2.9	0.86
Polypropylene-2 (PP30875)	(Elf Atochem)	0.30	0.09	0.042
Polypropylene-3 (PP1001)	(Solvay)	30	9.1	2.4
Polypropylene-4 (PP3808)	58000 (Solvay)	1.2	0.39	0.083
Ethylene-propylene (EP)	86000 (Exxon)	20	7.8	3.9
Amorphous nylon (PA330)	(DuPont)	70	35	0.84
Ethylene-propylene-maleic anhydride (EP-MA)	84000 (Exxon)	29	10	1.1
Polystyrene-oxazoline (PS-Ox)	200000 (Dow)	7	3.4	0.5

sheet of mercury without unwettable particles and these holes originated from point disturbances surrounded by ripples[21].

It was later established that perforations occurred in sheets of water containing sodium lauryl sulfate because of lauryl alcohol which was present as an impurity in the commercial grade sulfate[26]. However, it has been previously reported by Fraser *et al.*[27] that holes occurred in flat sheets of distilled water with no impurities. Additionally, the effects of air friction were diminished using a vacuum chamber. The authors indicated that there was no apparent reason for the distilled water sheet to break up via hole formation and hole growth.

It was also shown[27] that since the perforation not only has a radial velocity component but also one due to the diverging radial streamlines, the hole is more curved in the flow direction (away from the nozzle) and flattened in the opposite direction. More recently, holes were seen in liquid sheets and shown to produce a bimodal distribution of drops through breakup of thick ligaments perpendicular to the flow direction and thin ligaments parallel to the flow direction[28]. The work also showed that surface tension brings together the outer rims of the sheet. This convergence of the rims causes a wave to emanate from each rim, and when these waves interfere with each other there are thick and thin spots in the sheet. Point disturbances were seen but were attributed to vapour bubbles created by cavitation. The work on breakup of Newtonian liquid sheets shows that several breakup phenomena are possible and gives us insight into how breakup may occur during the initial stages of polymer blending. It was seen that flowing Newtonian liquid sheets can break up by forming holes which grow and coalesce with each other. The cause of the holes was explained partially by the presence of impurities; however, there are other causes which have not been discovered.

Instabilities in polymer sheets

Though some of the results in the previous section are similar to those we have obtained, polymer melts often do not behave like Newtonian fluids except at very low shear rates. Studies have been done on instabilities in viscoelastic multiphase flows. Schrenk and coworkers studied coextruded multilayer structures[29,30] and showed that there can be interfacial flow instability at a critical shear stress[31]. They showed that waves are formed at the interface and these waves can be stretched and folded when the instability becomes severe. Other work has clearly shown this instability, and has also shown that wave cresting occurs under harsh conditions[32]. Obviously, elasticity is important for determining flow stability. Thus, for sheet breakup, it will be important to look at the elastic moduli of the materials under the processing conditions. Theoretical work by Li on multilayer Couette flow[33] indicates that elasticity usually destabilizes the flow. Li suggested that elasticity would not play a role when the viscosities were matched. However, Chen points out that Li's result was due to an error in the shear stress[34] interface condition used in Li's analysis which did not account for the jump in the first normal stress across the interface. Chen[35] also showed that in multilayer Poiseuille flow, the cross-sectional volume of the more elastic component must be greater than a critical value to induce stability. The critical value is 32% when the more elastic component is in the core and 68% when it is in the annulus. Larson has given a good review of instabilities in viscoelastic flows[36].

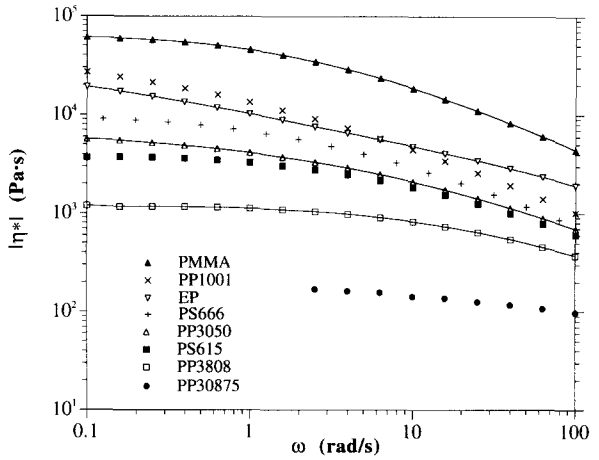

Figure 3 Complex viscosity ($|\eta^*|$) *versus* frequency (ω) for non-reactive systems at 200°C

The formation of holes in a thin polymer sheet inside a fluid matrix has not been reported except by our group[7,8]. However, work has been done on dewetting of thin spin-cast polymer films[37] on glass which gives a similar morphology to that observed by our group. Holes formed in the thin film, and the holes grew until they coalesced with each other to form a network of droplets. This breakup was postulated to occur via spinodal decomposition[37] and it was suggested that films thicker than approximately 100 nm did not break up by this mechanism. We do not believe that spinodal decomposition is the appropriate mechanism for sheet breakup in polymer/polymer blends. However, it is interesting that the hole patterns in the sheets reported by Reiter[37] are similar to those we have observed (*Figure 1* or *2*).

The quiescent breakup of a polymer sheet inside another polymer was studied by Elemans[20]. He microtomed a thin polymer sheet from a pellet and embedded it inside another polymer. He found that a sheet of dispersed phase broke up by forming threads and drops at the edges – the so-called 'fingering' mechanism. His micrographs seem to show that the ligaments formed from one hole, but he did not report this and it could not be unambiguously interpreted from the results presented. Since microtoming can give wavy, irregular sheets, the breakup mechanism may be different from that for affinely stretched, smoother sheets.

EXPERIMENTAL

Materials

All materials were commercial polymers provided in pellet form. The acronyms, suppliers, molecular weights and the flow properties of the materials are listed in *Table 1*. The dynamic rheological characterizations were performed using a Rheometrics RMS 800 rheometer with parallel plate fixtures. Two non-reactive polystyrenes were used in the experiments: Dow Styron 666D (PS666D) and Dow APR615 (PS615). PS666D is reported to have a melt index of 7.5 and PS615 has a melt index of 28. Two polypropylenes obtained from Elf Atochem, PP3050 and PP30875, and two polypropylenes obtained from Solvay, PP1001 and PP3808, were also used. PP3808 has a narrower molecular weight distribution than the other polypropylenes, and it will be interesting to see the effect that this has on breakup. Poly(methyl methacrylate) was obtained from Rohm and Haas. The ethylene-propylene rubber (EP) was Exxon EPV805 which has a 76% ethylene content. The complex viscosities ($|\eta^*|$) and the dynamic elastic moduli (G') are plotted *versus* frequency in *Figures 3* and *4*, respectively. The first normal stress difference N_1 can be approximated by $2G'$ at low shear rates.

The reactive polystyrene RPS XUS40056.01 (PS-Ox) was provided by Dow and is a copolymer of styrene and 1.0% oxazoline. The reactive ethylene-propylene copolymer (EP-MA) obtained from Exxon was EPXX1301, and it is a 0.7% maleic anhydride grafted material. The amorphous nylon was Zytel 330 (PA330) which was obtained from DuPont, and it is reported to have amine termination.

Procedure

Before moulding, the pellets of all the polymers used in the experiments were dried overnight in a vacuum oven at 90°C to remove any volatiles which could cause air bubbles upon heating. After drying overnight, two 25 mm diameter discs of matrix polymer were prepared in a heated plate press at a temperature of 200°C using a 1 mm thick aluminium spacer with 25 mm holes. Initially, low pressure (~20 kPa) was used to allow the molten polymer to flow and fill the holes in the spacer. Then the pressure was rapidly increased to 3 MPa and the press was cooled to room temperature within 3 min under pressure to prevent air bubbles from forming in the discs. To make a 'drop' of dispersed phase, a pellet of the dispersed phase polymer was cut into a cube of approximately 1 mg mass using a razor blade.

A Rheometrics RMS 800 rheometer with a 25 mm parallel plate fixture was used to study the morphology development in polymer blends under well-controlled simple shear conditions. The sample configuration is shown in *Figure 5*. One 25 mm diameter polymer disc was placed on the bottom parallel plate fixture. Three pellets of the same polymer were placed on top of the disc around its perimeter and the 1 mg dispersed phase pellet was placed on the disc 5 mm from its centre. The

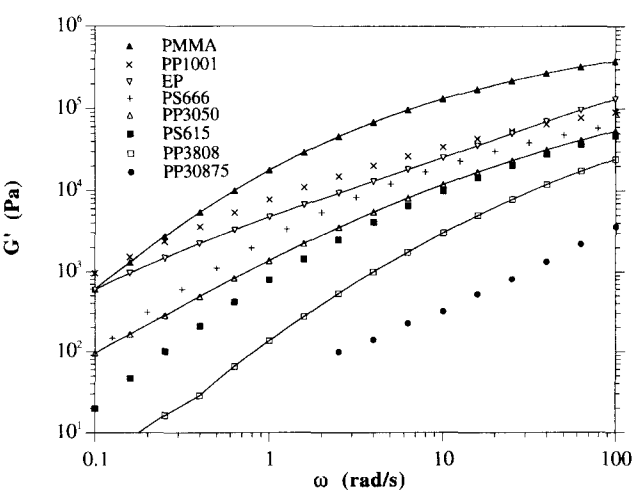

Figure 4 Dynamic elastic modulus (G') *versus* frequency (ω) for non-reactive systems at 200°C

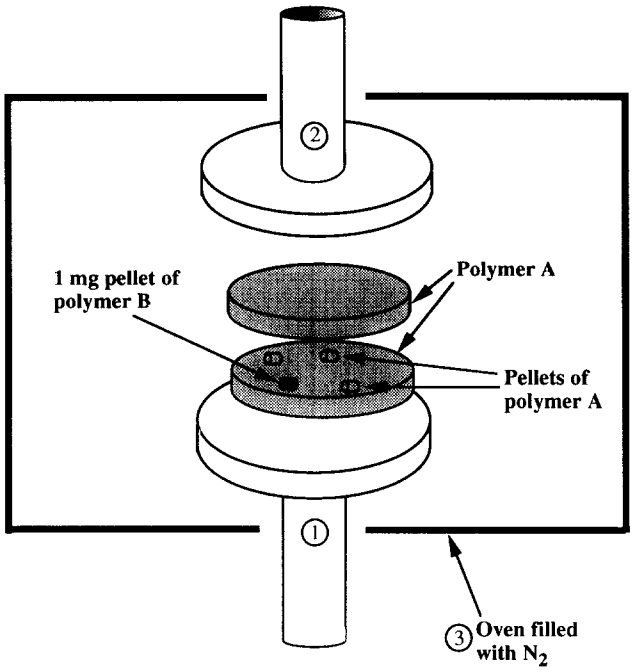

Figure 5 Sample preparation set-up for blending between parallel discs, showing (1) the rotating lower plate, (2) the stationary top plate and (3) the oven with nitrogen purge. The dispersed phase pellet ~1 mg (dark) is placed between the moulded discs of the matrix phase (shaded). Pellets of matrix phase are also used to flow around the pellet to minimize air bubbles when the discs are pressed together at high temperature

second 25 mm disc was placed on top of the three pellets and the gap between the two parallel plates was closed slowly until the upper plate just contacted the upper polymer disc. The rheometer oven, continuously purged with nitrogen gas to lessen polymer degradation, was used to heat the sample to 200°C. The gap between the parallel plates was then closed to 2.5 mm. The oven was opened and excess polymer was removed from the edge of the plates with a razor blade. The plates were then closed to a gap of 2 mm and an enclosing metal band was placed around the sample to prevent edge failure during blending. Then the sample was again heated to 200°C. The total loading time was approximately 5 min before shearing was started.

The blending was done by rotating the lower parallel plate at 0.01–8 rad s^{-1}. The rotation rate and mixing time were chosen so that the total strain was constant at 300. The base rotation rate and mixing time were 2 rad s^{-1} and 60 s, respectively. The systems and runs are summarized in *Table 2*. The interfacial tensions in the non-reactive polymer systems studied were found using the breaking thread method[20,38]. The interfacial tension in the PS/PP systems was 5 mN m^{-1}; in the PS/PMMA systems it was 1.5 mN m^{-1}; and in the PS/EP systems it was 4.5 mN m^{-1}. At different rotation rates, the mixing time was set to maintain a constant strain. At the end of mixing, the sample was cooled to room temperature using liquid nitrogen. The time required to freeze the sample morphology was approximately 1 min. The polymer sample was easily removed from the rheometer as a 2 mm thick disc. The surface of the disc was polished with Novus plastic polish for optical microscopy.

For some samples, the thicknesses of the sheets of the dispersed phase obtained by blending were found by breaking the polymer disc perpendicular to the shear direction. The piece was smoothed with sandpaper and faced with a Leica microtome until we obtained a flat, smooth surface which showed the cross-section of the polymer sheet. The sheet thickness was measured using an Olympus BHSM optical microscope.

RESULTS

Figure 6a shows a 1 mg PP3050 pellet which has been sheared inside a PS666D matrix. The morphology of the pellet after mixing at 2 rad s^{-1} ($\dot{\gamma} = 5\ s^{-1}$) for 80 s is shown in *Figure 6a* and the sheet breakup mechanism can be seen more clearly in the close-up shown in *Figure 6b*. The lacey sheet morphology parallels what is seen in the initial stages of blending in the batch mixer and the twin-screw extruder (see *Figures 1* and *2*). *Figure 6a* shows two sheets which have been pulled off the pellet and stretched thin enough for toroidal holes to form. The holes have coalesced and the sheet has disintegrated into droplets and ligaments. It can be seen that the holes form at the edges and then occur in the middle of the

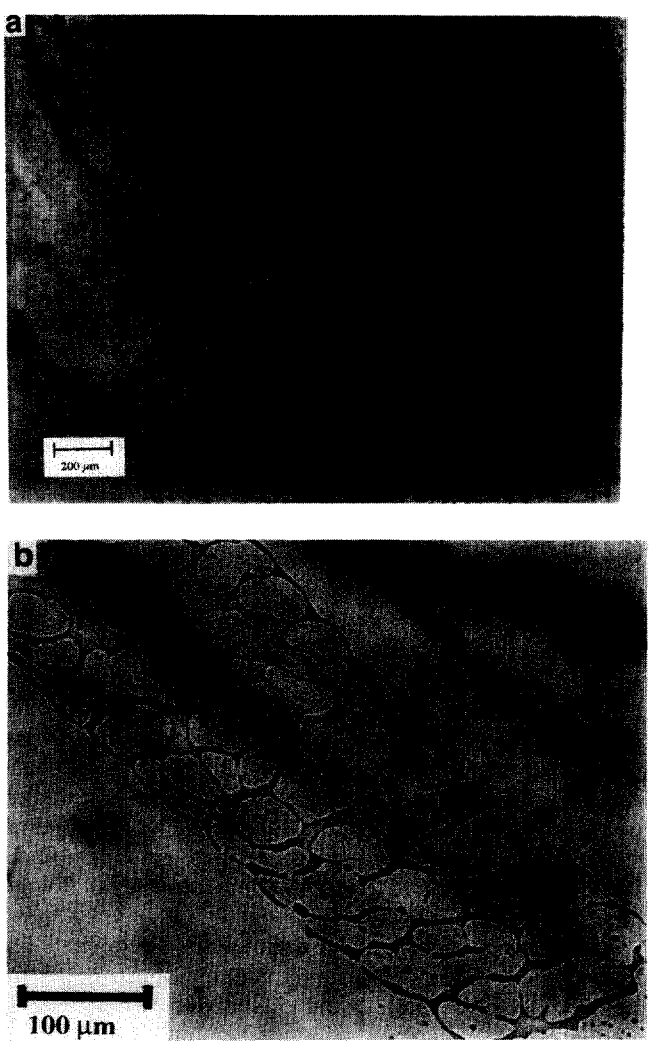

Figure 6 (a) Top view of a pellet of PP3050 that has been stretched by simple shear flow in the parallel discs geometry to form sheets which break up by forming holes ($T = 200$°C, $\dot{\gamma} = 5\ s^{-1}$, 80 s mixing). (b) Close-up of the region shown in the square in (a). The arrow indicates the shearing direction

Table 2 Polymer systems used for parallel plate blending experiments (total strain = 300; temperature = 200°C)

System (major/minor)	Shear rate (s^{-1})	G'_m (kPa)	G'_d (kPa)	*De*	Morphology[a]
PS666D/PP3050	0.125	0.15	0.13	0.11	cyl
	1.0	2.6	1.4	0.85	cyl
	5	12	6.7	4.3	sht/cyl
	20	30	20	17	sht
PS666D/PP30875	0.05	0.03	0.003	0.0021	cyl
	0.5	1.1	0.023	0.021	sht/cyl
	5	12	0.18	0.21	sht
PS666D/PP1001	1.25	3.4	9.2	3.0	cyl
	5	12	24	12	cyl
	10	20	34	24	sht/cyl
	20	30	49	48	sht
PS666D/PMMA	1.25	3.4	23	1.6	cyl
	2.5	6.7	47	3.1	cyl
	5	12	82	6.3	cyl
PS615/PP3050	1.0	0.8	1.4	0.87	cyl
	5	5.2	6.7	4.3	cyl/sht
	10	9.9	12	8.7	sht
PMMA/PS666D	0.083	0.43	0.08	0.05	cyl
	0.38	4.9	0.77	0.24	cyl/sht
	5	82	12	3.2	sht
	12.5	150	23	8	sht

[a] cyl = cylinder, sht = sheet; when both are listed, the first morphology is dominant

sheet. Holes that form near the edge of the sheet are halted by the sheet rim and when breakup occurs, the rim disintegrates into a string of drops. *Figure 6b* shows that parallel to the flow direction, the ligaments formed between coalescing holes are stretched out and broken into droplets, micrometres in size. However, perpendicular to the flow direction, thick ligaments have formed and these ligaments remain. It should be noted that the time required to freeze the morphology was about 1 min and the morphology probably changed during this time. However, the breakup mechanism is clear.

The cross-section of the sheet perpendicular to the flow direction was also viewed. The edges of the sheet (the rims) are thicker than the inner portion of the sheet. The samples where holes were seen had sheets of thickness between 2.0 and 25 μm, but the locations seen in the cross-section may not have been the same locations where holes were seen. Therefore, the actual part of the sheet that formed holes was probably thinner than 25 μm and was closer to 1.0 μm in thickness. *Table 2* lists the systems studied, the corresponding shear rates, elastic moduli, Deborah numbers and the types of morphology that were created.

Using simple shear in the parallel discs geometry, we investigated different factors affecting sheet breakup, namely (1) shear rate, (2) the elastic/viscosity ratio and (3) the effect of reaction. All runs were standardized by maintaining a constant total strain of 300 and were performed at a temperature of 200°C. The effect of increasing rotation rate was investigated for the PS666D/PP3050 (matrix/pellet) system and the results are shown in *Figure 7*. The rotation rate was increased from 0.05 to 8 rad s^{-1}. The corresponding shear rates were found by multiplying the rotation rate by 2.5 because of the sample geometry, so the shear rates here varied from 0.125 to 20 s^{-1}. At constant strain, the pellet forms sheets more readily when the shear rate is increased. At very low shear rates, the materials act like Newtonian fluids and the pellet is deformed into a cylinder (see *Figure 7a*). Interfacial forces are important enough here to bring together the edges of a ribbon or sheet. As the shear rate is increased to an intermediate value, we see that the PP3050 pellet forms sheets but these sheets are not thin enough to form holes. Instead, they break up only at the front edges where they are thinnest. Once the shear rate is increased to 20 s^{-1}, thinner sheets are formed and these sheets break up via hole formation. Again, it should be noted that about 1 min was required to quench the polystyrene matrix below its glass transition.

Pellets of four polypropylenes (1–4 in *Table 1*) with different rheological properties were sheared at 2 rad s^{-1} for 60 s inside a PS666D matrix at 200°C. The complex viscosities of the materials ($\eta^*(5\ s^{-1})$), which combine both the elastic and loss moduli, were used to calculate the viscosity ratios shown in *Figure 8*. The viscosity ratio is defined as $\eta_r = \eta_d/\eta_m$, where η_d is the pellet phase (or dispersed phase) viscosity and η_m is the matrix phase viscosity. Decreasing the viscosity ratio allows the matrix to stretch out the dispersed pellet more easily. The morphology changes from cylinders to sheets which break up via hole formation as η_r decreases. Surprisingly, the PS666D/PP3808 system ($\eta_r = 0.3$) showed breakup comparable to the lowest viscosity ratio system, i.e. PS666D/PP30875 ($\eta_r = 0.06$). Moreover, the PS666D/EP system

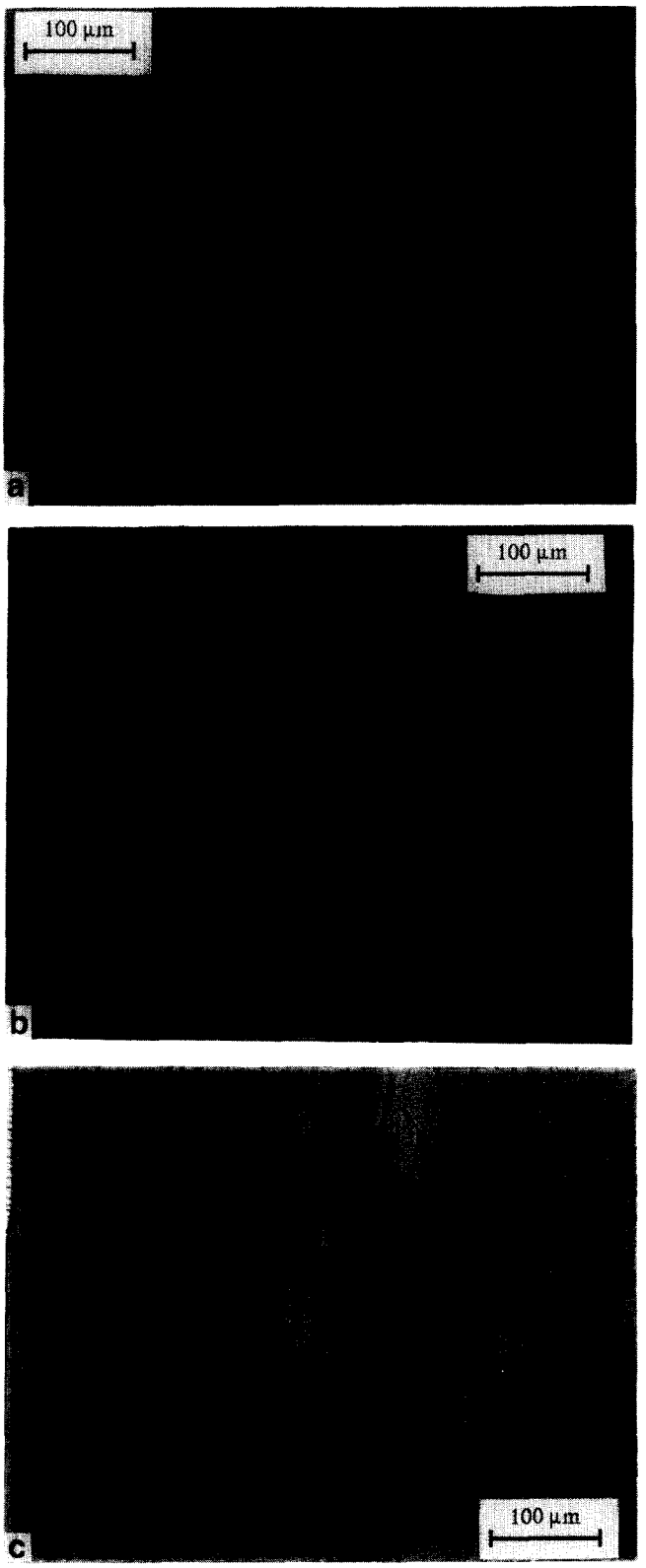

Figure 7 Photographs showing the effect of shear rate for a PP3050 pellet which breaks up inside a PS666D matrix at 200°C. (a) At $\dot{\gamma}=0.125\,s^{-1}$ (2400 s of mixing), the PP3050 pellet is stretched out into a cylinder. (b) At $\dot{\gamma}=5\,s^{-1}$ (60 s of mixing), a sheet is formed which breaks up only at the edges. (c) At $\dot{\gamma}=20\,s^{-1}$ (15 s of mixing), holes are formed at the edges of the sheet

(see *Figure 9a*), which had a viscosity ratio greater than 2, also broke up the same way. The reason for this will be explained later in this paper. Note that the micrograph in *Figure 8c* is the same as *Figure 7b*. The micrograph is purposefully shown twice since it shows the transition region between cylinders and sheets with holes.

The effect of reaction at an interface during blending was investigated and the morphologies of the PS666D/EP and PS-Ox/EP-MA systems blended at 2 rad s^{-1} ($\dot{\gamma}=5\,s^{-1}$) for 60 s are shown in *Figures 9a* and *9b*. The uncompatibilized PS666D/EP system shows breakup similar to the lower viscosity ratio PS/PP systems; however, the reactive EP-MA pellet shows no breakup (*Figure 9b*) at the same shear rate. This was surprising since the non-reactive and reactive PS/EP systems have similar rheological properties. However, when blended at a higher shear rate ($\dot{\gamma}=28\,s^{-1}$) for the same time, the EP-MA pellet does break up. The morphology is shown in *Figure 9c*. It is important to mention that in our experiments, contrary to most polymer/polymer blending operations, the two materials were contacted at processing temperatures when no shear was applied. Thus, reaction can occur before blending and affect subsequent morphology development. Though it is not directly applicable to morphology development in reactive blends, the result shows that interfacial copolymers formed by reaction stabilize the blend structure. At the same shear rate, the reactive pellet was hardly deformed, whereas the non-reactive pellet had been stretched into a thin sheet with holes. We suggest that the reaction increases the interfacial viscosity owing to reactively formed copolymers, and that these copolymers form an elastic shell around the pellet making it more difficult to deform the reactive pellet. It should be noted that the PS-Ox/EP-MA system, like many commercial systems, can crosslink at the interface.

DISCUSSION

Sheet breakup

We performed experiments[38] on the breakup of a polymer sheet in a quiescent polymer matrix at processing temperatures (over 200°C). The results for a PS666D sheet inside a PMMA matrix showed that spin-cast sheets broke up inside a polymer matrix without any external shear. The PS666D sheets were made by spin casting on glass and then annealed at T_g and then floated on water. The sheet was then picked up using a PMMA slab which had been prepared by compression moulding. Another PMMA slab was placed on top of the sheet and the sample sandwich was placed between two cover slips. The stresses due to spin casting radiate outward from the centre of the sheet. Even though the sheets were annealed at the glass transition temperature, stresses may have remained in the sheets since they adhered to the glass substrate. When placed in the Mettler FP82 hot stage that was used to heat the sample under the microscope, the stress in the sheet could completely relax at the processing temperature of 200°C. The sheet contracted from the edges and this could have caused flow and perhaps generated interfacial waves on both the top and bottom surfaces. If troughs from waves on either side of the sheet touched, then a hole would form and grow to minimize the interfacial area.

To avoid any solvent effects, the quiescent sheet breakup was studied using a 10 μm thick sheet which had been prepared by melting and squeezing at high

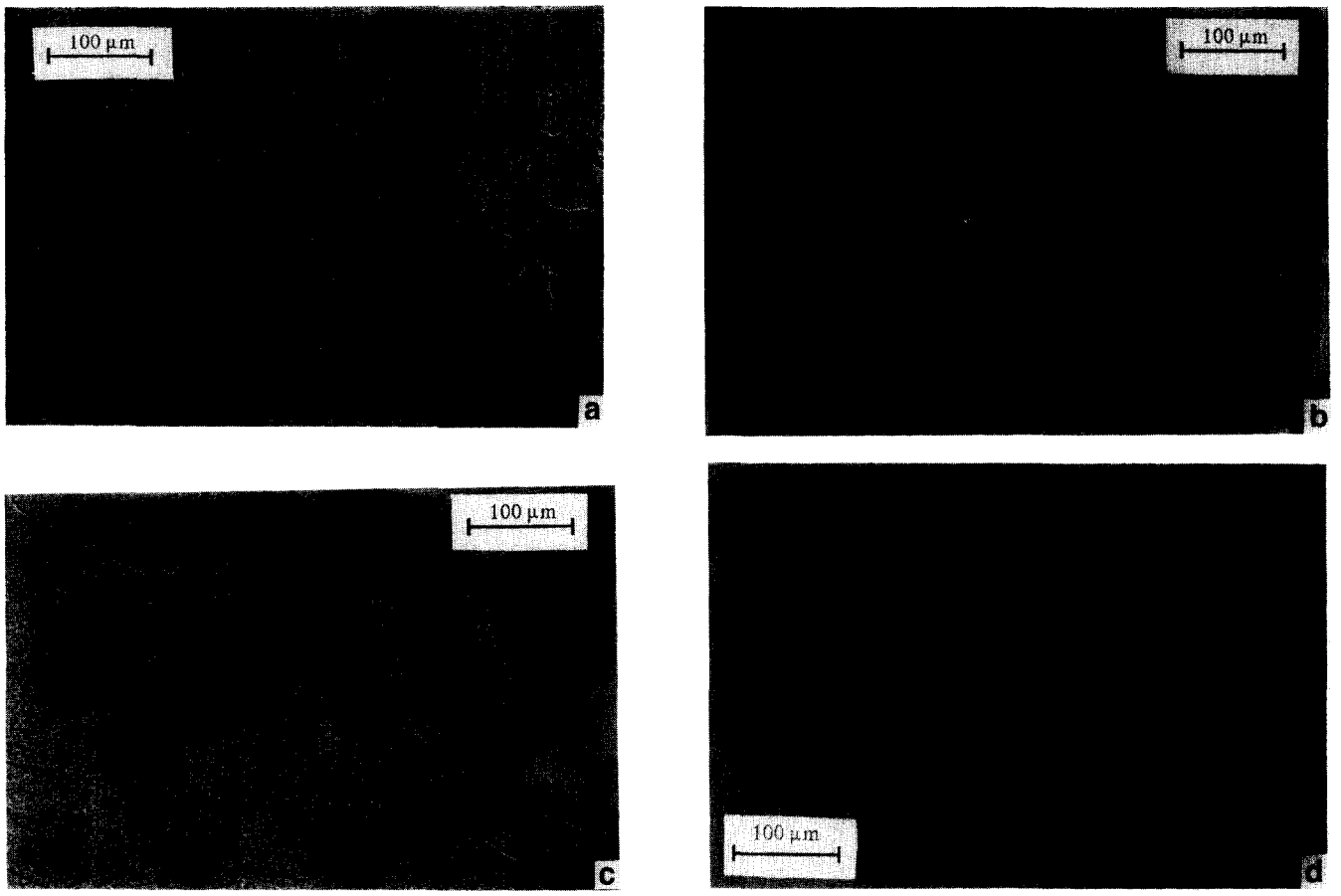

Figure 8 Photographs showing the effect of viscosity ratio for changing PP viscosity. Different PP pellets break up inside the PS666D matrix at 200 C and $\dot{\gamma} = 5\ s^{-1}$ (60 s of mixing). (a) For PS666D/PP30875 ($\eta_r = 0.06$), the pellet is stretched out into sheets which break up by forming holes. (b) For PS666D/PP3808 ($\eta_r = 0.3$), sheets with holes are formed. (c) For PS666D/PP3050 ($\eta_r = 0.9$), a sheet is formed which breaks up at the edges. (d) For PS666D/PP1001 ($\eta_r = 2.0$), a large cylinder of PP is formed. It is shown in the Discussion section that the viscosity ratio is not the key parameter controlling breakup

pressure in a plate press. A PS666D pressed sheet was placed between two PMMA plates and the sandwich was heated to 230°C in the hot stage. After 1 h, no breakup was observed. The sample was taken out of the hot stage for a few seconds and sheared by sliding the cover slip on top of the sample, which generated about 100% strain. When the sample was replaced in the hot stage, breakup by hole formation occurred almost immediately. The compression-moulded sheet, which was not stuck to glass during annealing, may have relieved stresses more easily and thus did not break up even at a higher temperature. However, once shear stress was imposed manually, the sheet broke up immediately. It is concluded from these experiments that the sheet must be sheared and then allowed to relax for holes to form.

In industrial polymer blending, flow is imposed using an intensive mixer which has both shear and extensional components. The model experiments show that a polymer sheet can be formed inside a matrix of another polymer in a simple shear field. Extensional flow was not required to obtain sheets. Simple shear between parallel discs was used to evaluate the important factors governing the breakup mechanisms. Holes formed at a sheet thickness between 2 and 25 μm. At this length scale, interfacial tension will be important (interfacial stress $\sim 10^3$ Pa) and will cause the sheet to contract and form rims at the edges. It is speculated that when the sheet is thin enough, dimples formed on either side of the sheet by interfacial waves allow the two surfaces to touch and form a hole. Other viscoelastic instabilities[32] may also occur. A cross-section of the PP3050 sheet inside the PS matrix is presented in *Figure 10*. The cross-section in *Figure 10* is perpendicular to the images shown in *Figures 6*, *7* and *8*. The cross-section shows that the sheet becomes thinner in the radial direction. Therefore, for the parallel plate experiments, the radial shear rate gradient has some importance.

It had been previously thought that for a sheet to form, a solid pellet needed to be sheared against a hot surface[7]. However, we have shown that sheets are generated even if both phases are melted and the pellet is inside the matrix. Therefore, rather than being a melting phenomenon, sheeting is related to the material properties. This does not imply that melting does not play a role. One can visualize a pellet that melts at the surface and the melted portion is pulled off as a sheet. The sheet will continue to grow as more of the pellet melts and feeds the sheet. Melting of a pellet during mixing was not studied in these model experiments; however, it is possible to ramp the temperature so that the pellet will melt during the shearing.

Analysis

It has been shown that increasing the shear rate, which increases the matrix shear stress, causes a change in the

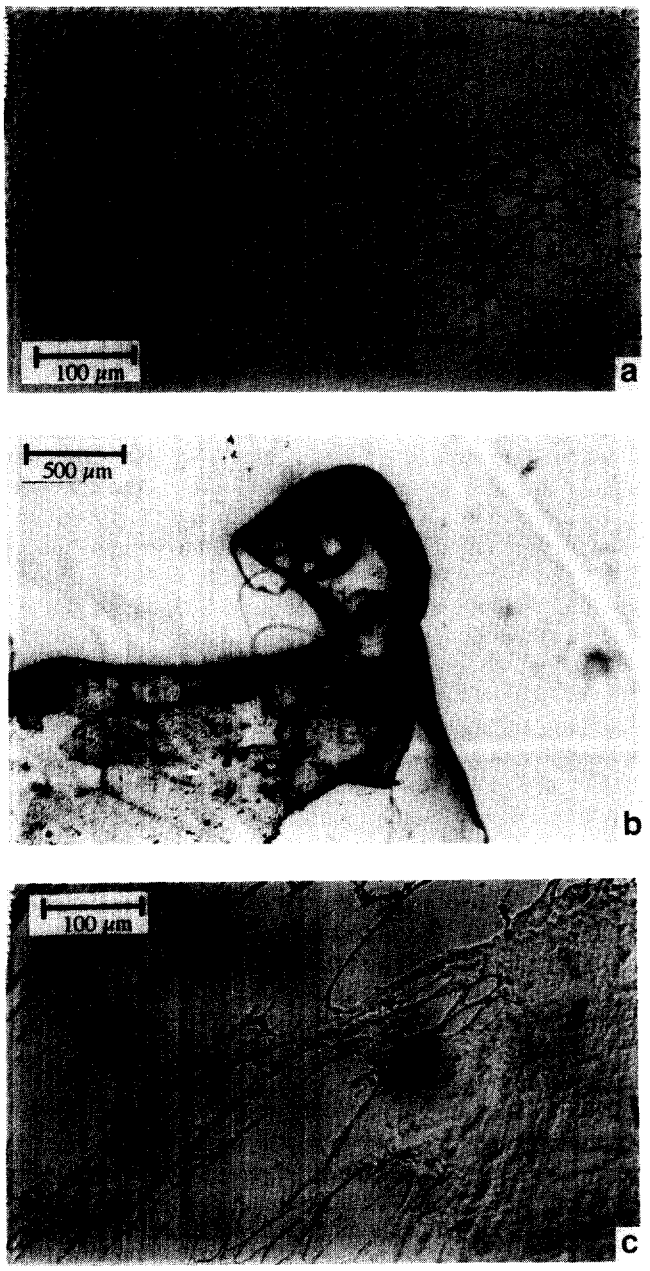

Figure 9 Photographs showing the effect of reaction at 200°C (60 s of mixing). (a) For the uncompatibilized PS666D/EP system ($\dot{\gamma} = 5\ s^{-1}$), the breakup via hole formation is very similar to what is seen in the lower viscosity ratio PS/PP systems. However, the viscosity ratio here is 2.4. (b) For the reactive PS-Ox/EP-MA system at $\dot{\gamma} = 5\ s^{-1}$ ($\eta_r = 2.7$), the EP-MA pellet has only been slightly deformed (note the lower magnification). (c) For the reactive PS-Ox/EP-MA system at $\dot{\gamma} = 28\ s^{-1}$, the EP-MA does break up. Note, though, that the overall strain is 5.6 times as high

breakup mechanism (*Figure 7*). At a high shear rate, the sheets are thinned out and break up into small particles by hole formation, whereas at lower shear rates the pellet is stretched out into a cylinder or a long ribbon and cannot be broken up as efficiently. On changing the viscosity ratio (*Figure 8*), we see that decreasing the viscosity ratio encourages sheet formation. At a high enough viscosity ratio, only a cylindrical morphology is observed. Therefore, we tried to represent the data using the capillary number and the viscosity ratio $\eta_r = \eta_d/\eta_m$, where η_d is the dispersed phase viscosity and η_m is the matrix viscosity. The capillary number is given by

$$Ca = \frac{\eta_m \dot{\gamma} r}{\Gamma} \tag{1}$$

where $\dot{\gamma}$ is the shear rate, r is the 'radius' of the pellet or initial drop and Γ is the interfacial tension. Ca and η_r have been used to describe drop breakup in Newtonian systems.

Two discrepancies occurred when we analysed the experiments using Ca and η_r. The first was that the transition from low shear rate to high shear rate for different systems could not be explained. Moreover, as we increased the viscosity ratio, the behaviour of the PS666D/PP3808 and PS666D/EP systems was not consistent with other results (see *Figures 8* and *9*). As mentioned previously, PP3808 had a narrow molecular weight distribution and showed significantly different elastic behaviour. Even at processing temperatures, polymers have a large elastic component, especially at the high shear rates in a twin-screw extruder, but also in our model experiments. The breakup phenomena involve deformation of a viscoelastic material by a viscoelastic material, and therefore we decided to incorporate the first normal stresses of the materials and the relaxation time of the pellet phase in the analysis.

The matrix normal stress $T_{11.m}$ will deform the 'pellet' phase into a sheet and this will be resisted by the normal stress of the pellet $T_{11.d}$ and the interfacial tension, which will try to keep the interface curved. T_{11} can be approximated by the first normal stress difference $N_1 = T_{11} - T_{22}$, since generally $T_{11} > T_{22}$. Therefore, we can write a ratio of the breakup force and the restoring force as

$$\frac{N_{1.m}}{N_{1.d} + \Gamma/r} = \frac{\text{breakup force}}{\text{restoring force}} \tag{2a}$$

The first normal stress difference N_1 is approximately $2G'$ at low shear rate or frequency, where G' is the elastic

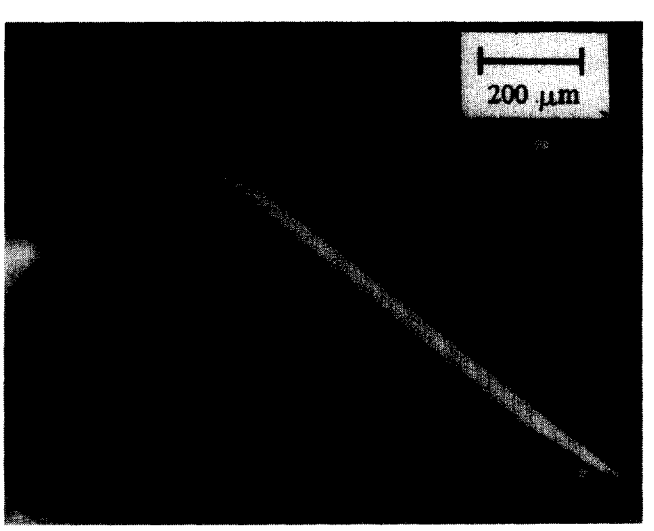

Figure 10 Photograph showing a cross-section of the PS666D/PP3050 system at $\dot{\gamma} = 5\ s^{-1}$ (60 s of mixing). The PP sheet is white and the PS matrix is black when side lighting is used. The sheet thins as we move radially outward (the arrow shows the radially outward direction). This is probably due to a higher shear rate at the outer edge and could also be due to secondary flows

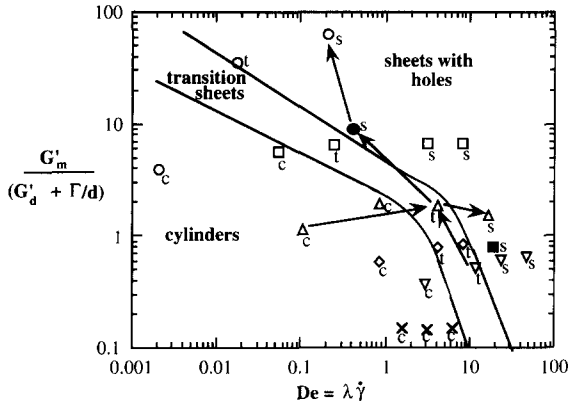

Figure 11 Map of breakup for sheared then quenched samples for a total strain of 300. The letters denote the morphology at each point: s, sheets with holes; t, transition between cylinders and sheets; c, cylinders. As the Deborah number and the ratio of drop breakup forces to drop-restoring forces increases, the pellet is stretched into thinner sheets. At low enough values of the two controlling parameters (in the bottom left corner), only cylinders are seen. In this corner, interfacial forces dominate and pull together the edges of the sheet. Different symbols denote different systems: (○) PS666D/PP30875; (□) PMMA/PS666D; (△) PS666D/PP3050; (◇) PS615/PP3050; (▽) PS666D/PP1001; (×) PS666D/PMMA; (●) PS666D/PP3808 (sheets with some holes); (■) PS666D/EP (sheets with holes). The scans in *Figures 7* and *8* are shown by the arrows

modulus. The ratio in equation (2a) becomes

$$\frac{\text{breakup force}}{\text{restoring force}} = \frac{G'_m}{G'_d + \Gamma/d} \tag{2b}$$

where d is the diameter of the pellet or drop. The ratio in equation (2b) will be termed the 'stress ratio' in the rest of this paper. Pellet breakup is also controlled by the rate of deformation of the pellet phase and its rate of relaxation. If it relaxes quickly in comparison to the process time, then we would expect the deformation to be more like the Newtonian case (where the relaxation time is zero). However, if the pellet phase relaxes slowly in comparison to the process time, the deformation will be more elastic. The ratio of the relaxation time of the material to the characteristic process time is expressed as the Deborah number

$$De = \lambda\dot{\gamma} \tag{3}$$

where λ is the characteristic relaxation time of the pellet phase (see *Table 1*) and $\dot{\gamma}$ is the shear rate. The characteristic relaxation times were found from the complex viscosity *versus* frequency data shown in *Figure 3*. The crossing of the line representing the zero shear rate viscosity and the line representing the power law viscosity at high frequency was used to find the critical frequency ω_c, and $\lambda = 1/\omega_c$. The map showing how these two parameters affect the breakup mode is shown in *Figure 11*.

It is seen that when the matrix normal stress is low enough compared to the sum of pellet normal stress and interfacial stress, only cylinders are formed. As the relaxation time of the pellet phase decreases, it becomes more difficult to create a sheet. At intermediate stress ratios and Deborah numbers, the cylinders are flattened to give sheets which break up only at the edges. At the higher stress ratios and Deborah numbers, the sheet breaks by hole formation. A consistent map representing the different systems is obtained for a wide range of processing conditions. The map shows about a three orders of magnitude change in both the stress ratio and the Deborah number. The discrepancies in the Ca–η_r analysis of the PS666D/PP3808 and PS666D/EP systems are not observed in *Figure 11*, and these two points are shown by filled symbols. Since PP3808 has a very narrow molecular weight distribution, there are very few very long chains. Therefore, the relaxation time for PP3808 (see *Table 1*) is similar to that for PP30875. Therefore, although the PP3808 viscosity is six times as large, its relaxation time is only twice as long as that of PP30875. The PP3808 data point is depicted between the 'transition sheets' region and the 'sheets with holes' on the map (*Figure 11*), and since sheets with some holes were observed, this point also fits in the analysis. The relaxation time of the EP is comparable to that of the PP3050 phase, although the EP viscosity is 2.5 times the PP3050 viscosity. EP would be expected to form cylinders since the viscosity ratio is the same as that in the PS666D/PP1001 system in *Figure 8d*. However, the G' of EP is similar to that of PS666D, even though the viscosity ratio is 2.4. Thus, the breakup mode of the PS666D/EP system is predicted in *Figure 11* to be more like that of the PS615/PP3050 system. Therefore, we can predict the breakup behaviour of non-reactive materials reasonably well if we know the rheological and interfacial properties of the materials and the size of the dispersed phase.

When the total strain was changed, the transitions between breakup modes changed. We obtained results for the PS615/PP3050 system at 150 total strain units and 600 total strain units (the data shown in *Figure 11* are at 300 total strain units) which showed that the transition lines shifted as the total strain was varied. Therefore, the transition lines in *Figure 11* are only valid for the total strain studied. Qualitatively, we observe that increasing the total strain shifts the transitions to the left (making it more easy for sheets to form) and decreasing the total strain shifts the transitions to the right in *Figure 11*.

The dependence of the breakup mode on the Deborah number has been investigated by Milliken and Leal for drops of polymer solution in a Newtonian matrix under planar extensional flow[39]. The calculation of the relaxation time was similar to what was used in this paper. They saw that as the Deborah number of the 'viscoelastic' drop increased, the mode of breakup changed from a stretched cylinder with bulbous ends which pinched at the centre to a drop with cusped ends which ejected a thin fluid thread. A Deborah number of 1 was seen experimentally as the transition from Newtonian to elastic behaviour. This work cannot be directly compared with our work since they used a Newtonian matrix and a different flow field. Moreover, they did not use polymer melts which can have much longer relaxation times. However, they did identify that the elastic properties of their materials determined the breakup phenomena.

The stress ratio shown in equation (2b) can be used to show that since the pellet size is large enough that we have a low interfacial stress compared to the first normal stress differences of the polymer systems studied in this paper, these breakup experiments are equivalent to a Newtonian drop breaking up inside a Newtonian matrix

with zero or very low interfacial tension. For Newtonian systems, zero interfacial tension can be achieved by placing a coloured drop inside a matrix of the same fluid. Thus, if the top of the system is moved to induce planar shear flow, the drop will be affinely stretched in the direction of the streamlines. In addition, the end of the drop closest to the moving surface will be displaced further than the opposite end, causing the drop to be oriented at some angle (small at high deformations) from the flow direction. The reason that sheets form in our system is clear; at the millimetre scale (most pellets are a few millimetres in size), the interfacial stresses on the drop are negligible compared to the normal stress and the viscous stress. Therefore, the pellet will be stretched as if it was part of the matrix. Curved interfaces should not be observed until the length scale is of the order of a micrometre in size since only then will the interfacial stress be as important as the shear stress. This reasoning is supported by results like those in *Figure 10*, where domains larger than 20 μm in size are shown to be compressed sheets stretched in the flow direction.

Morphology

We also performed direct visualization experiments using a video camera and a transparent parallel plate mixer[38,40] with the same sample geometry as shown in *Figure 5*. The apparatus could be heated to processing temperatures. A complete description of the apparatus is given elsewhere[40]. In the initial morphology development, lacey sheets and cylinders parallel to the flow direction were seen and these broke up into very small droplets. Thus, we can have an incredibly wide distribution of domain sizes from 1 to 100 μm during the initial blending stages. Moreover, two characteristic drop sizes can form since ligaments between holes parallel to the flow direction are stretched out and broken into small droplets, while the large cylinders perpendicular to the flow direction remain and eventually break into larger droplets (see *Figure 6*). This bimodal particle size distribution has been seen in polymer blends mixed for short times in internal mixers[7]. In industrial mixers, flow reorientation allows large particles to be broken up over time. There was no reorientation in our parallel discs, so the large cylinders persisted for longer times. It was also evident that circular holes were not present during blending; instead, the holes were flattened until they bridged the sheet to leave cylinders perpendicular to the flow field.

It should be emphasized that in our model studies, a uniform stress level was applied to the pellet throughout the breakup experiment. In an industrial mixer, such as a twin-screw extruder, the mixing blades, or kneaders, will have different clearances with the barrel. Therefore, the pellet will see at least two stress levels. Under high stress, the dispersed phase will be stretched out, say into a sheet, but it will relax in the lower stress region. It is the lower stress region that allows holes to form in the sheet as it relaxes. Therefore, it is important to have different levels of stress to have good dispersive mixing[41,42]. These mechanisms describe how millimetre-sized pellets break into submicrometre-sized particles within a few seconds' residence time in a twin-screw extruder.

Using the special visualization apparatus, it was shown that quenching times must be well within 15 s to preserve the morphology during mixing. Therefore, it is best to study mixing using 'on-line' visualization. Cylinders were stable as long as the flow was steady, but the cylinders quickly broke up via the Rayleigh instability[40,42,43] when the shear was stopped. Stable fluid cylinders under flow have been reported for Newtonian systems[42,44] and elasticity should make the cylinders more stable[45]. Cylinders should also break up more readily when there is a combination of different stress levels[41,42].

It was more difficult to deform the pellet in reactive systems (see *Figure 9*). This result contradicts the accepted concept in blend literature[16,46–51] that copolymers at the interface reduced interfacial tension, and therefore should make deformation of the dispersed phase easier. Our results suggest that if given enough time, reaction inhibits flow. It will be interesting to try to study breakup while the pellet is melting so that interfacial reaction occurs concurrently with the morphology development. The reaction may inhibit flow when the interface is covered with a shell of copolymer, but, on the other hand, if the functional groups diffuse to the interface and only some of the chains react to form copolymers, a very different breakup mechanism may be observed. It is thought that the breakup may be similar to the non-reactive case, but any small particles will be stabilized by the reaction against coalescence. Contrary to what is reported in most blend literature, we suggest that these small particles, once stabilized, will resist deformation owing to an increased interfacial viscosity. Recent results confirm our proposition of increased resistance to deformation when compatibilizers are added[52,53].

CONCLUSIONS

The results show that during blending, pellets of the dispersed phase are stretched out into sheets which break up into cylinders via different mechanisms. It is shown that at low enough shear rates, cylinders form from the pellet. This occurs because the sum of the normal stress of the drop ($T_{11,d}$) and the interfacial stress is comparable with the matrix normal stress ($T_{11,m}$), and the drop can resist being stretched into a sheet. A map showing the different regions of breakup was presented at one strain value using the ratio of the stresses and the Deborah number. It has been shown that this map predicts breakup behaviour in polymer blends well. As the Deborah number is increased, the pellet breakup is less like the Newtonian case and sheets are formed easily. When the strain is increased, the dividing lines between breakup modes shift, indicating that a three-dimensional map with total strain as the third variable will represent the breakup better.

It was demonstrated that sheets can be generated in simple shear fields, and if these sheets can be stretched thin enough, holes form in the sheets and grow until they coalesce to give ligaments both parallel and perpendicular to the flow direction. The perpendicular ligaments are thicker and will not break up unless there is flow reorientation. The cause of the holes is still undetermined, but it is inferred from the experiments that if the sheet is sheared and allowed to relax, then interfacial instabilities occur and cause interfacial waves which pinch the sheet and form holes.

Viscoelastic cylinders are stable in steady flows. A combination of stress levels is required for breakup such that the dispersed phase domains are affinely stretched in a high stress region and then allowed to relax and break up in a lower stress region. Interfacial reaction stabilizes the dispersed phase domains, and if the reaction forms a viscous, elastic shell around large drops, they will be difficult to break up.

ACKNOWLEDGEMENTS

We would like to thank R. A. Cairncross and R. Hanamanthu for useful discussions. This work was partially funded by NSF grant CTS-9203108. The authors are grateful to DuPont and 3M for financial support of this work. One of us (U.S.) is grateful to the Plastics Institute of America for supplemental scholarships during various periods of this research.

REFERENCES

1 Karger-Kocsis, J., Kalló, A. and Kuleznev, V. N. *Polymer* 1978, **19**, 448
2 Favis, B. D. *J. Appl. Polym. Sci.* 1990, **39**, 285
3 Plochocki, A. P., Dagli, S. S. and Andrews, R. D. *Polym. Eng. Sci.* 1990, **30**, 741
4 Shih, C. K., Tynan, D. G. and Denelsbeck, D. A. *Polym. Eng. Sci.* 1991, **31**, 1670
5 Dekker, M. E. J., Hobbs, S. Y., Bruker, I. and Watkins, V. H. *Polym. Eng. Sci.* 1990, **30**, 1628
6 Nishio, T., Suzuki, Y., Kojima, K. and Kakugo, M. *J. Polym. Eng.* 1991, **10**, 123
7 Scott, C. E. and Macosko, C. W. *Polym. Bull.* 1991, **26**, 341
8 Sundararaj, U., Macosko, C. W., Rolando, R. J. and Chan, H. T. *Polym. Eng. Sci.* 1992, **32**, 1814
9 Lindt, J. T. and Ghosh, A. K. *Polym. Eng. Sci.* 1992, **32**, 1802
10 David, B., Kozlowski, M. and Tadmor, Z. *Polym. Eng. Sci.* 1993, **33**, 227
11 van Oene, H. *J. Colloid Interface Sci.* 1972, **40**, 448
12 Heikens, D. and Bartensen, W. *Polymer* 1977, **18**, 69
13 Heikens, D., Hoen, N., Bartensen, W., Piet, P. and Ladan, H. *J. Polym. Sci., Polym. Symp.* 1978, **62**, 309
14 Danesi, S. and Porter, R. S. *Polymer* 1978, **19**, 448
15 Min, K., White, J. L. and Fellers, J. F. *J. Appl. Polym. Sci.* 1984, **29**, 2117
16 Wu, S. *Polym. Eng. Sci.* 1987, **27**, 335
17 Subramanian, P. M. *Polym. Eng. Sci.* 1985, **25**, 483
18 Subramanian, P. M. and Mehra, V. *Polym. Eng. Sci.* 1987, **27**, 663
19 Kamal, M. R., Hozhabr, S., Arhyris, L. and Lambla, M. *Soc. Plast. Eng. Tech. Pap.* 1992, **50**, 2677
20 Elemans, P. H. M. PhD Thesis, Technical University of Eindhoven, The Netherlands, 1989
21 Dombrowski, N. and Fraser, R. P. *Philos. Trans. R. Soc. London, Ser. A* 1954, **247**, 13
22 York, J. L., Stubbs, H. E. and Tek, M. R. *Trans. ASME* 1954, **75**, 1279
23 Simons, A. and Goffe, C. R. Power Jets Report R.1188, Aeronautical Research Council, 1946
24 Garrett, P. R. *J. Colloid Interface Sci.* 1979, **69**, 107
25 Taylor, G. I. *Proc. R. Soc. London, Ser. A* 1959, **253**, 313
26 Andrew, S. P. S., Damani, M. A. K. and Dombrowski, N. *J. Colloid Interface Sci.* 1972, **41**, 445
27 Fraser, R. P., Eisenklam, P., Dombrowski, N. and Hasson, D. *AIChE J.* 1962, **8**, 672
28 Mansour, A. and Chigier, N. *Phys. Fluids A* 1990, **2**, 706
29 Schrenk, W. J. and Alfrey Jr, T. *SPE J.* 1973, **29**, 38
30 Schrenk, W. J. and Alfrey Jr, T. *SPE J.* 1973, **29**, 43
31 Schrenk, W. J., Bradley, N. L., Alfrey Jr, T. and Maack, H. *Polym. Eng. Sci.* 1978, **18**, 620
32 Wilson, G. M. and Khomani, B. *J. Non-Newtonian Fluid Mech.* 1992, **45**, 355
33 Li, C. H. *Phys. Fluids* 1970, **13**, 1701
34 Chen, K. *J. Non-Newtonian Fluid Mech.* 1991, **40**, 261
35 Chen, K. *J. Non-Newtonian Fluid Mech.* 1991, **40**, 155
36 Larson, R. G. *Rheol. Acta* 1992, **31**, 213
37 Reiter, G. *Phys. Rev. Lett.* 1992, **68**, 75
38 Sundararaj, U. PhD Thesis, University of Minnesota, Minneapolis, 1994
39 Milliken, W. J. and Leal, L. G. *J. Non-Newtonian Fluid Mech.* 1991, **40**, 355
40 Sundararaj, U., Dori, Y. and Macosko, C. W. *Soc. Plast. Eng. Tech. Pap.* 1994, **52**, 2448
41 Grace, H. P. *Chem. Eng. Commun.* 1982, **14**, 225
42 Janssen, J. PhD Thesis, Technical University of Eindhoven, The Netherlands, 1993
43 Tomotika, S. *Proc. R. Soc. London, Ser. A* 1935, **150**, 322
44 Khakhar, D. V. and Ottino, J. M. *Int. J. Multiphase Flow* 1987, **13**, 71
45 Bousefield, D. W., Keunings, R., Marrucci, G. and Denn, M. M. *J. Non-Newtonian Fluid Mech.* 1986, **21**, 79
46 Utracki, L. A. 'Polymer Alloys and Blends', Hanser, Munich, 1989, p. 26
47 Paul, D. R. in 'Polymer Blends' (Eds D. R. Paul and S. Newman), Academic Press, New York, 1978, Ch. 12
48 Fayt, R., Jerome, R. and Teyssié, Ph. *Polym. Eng. Sci.* 1987, **27**, 328
49 Willis, J. M. and Favis, B. D. *Polym. Eng. Sci.* 1988, **28**, 1416
50 Chen, C. C., Fontan, E., Min, K. and White, J. L. *Polym. Eng. Sci.* 1988, **28**, 69
51 Scott, C. E. PhD Thesis, University of Minnesota, Minneapolis, 1990
52 Gonzalez-Nunez, R., Favis, B. D., Carreau, P. J. and Lavallée, C. *Polym. Eng. Sci.* 1993, **33**, 851
53 Datta, S. and Lohse, D. J. *Macromolecules* 1993, **26**, 2064